AAC 2017

AACHEN ACOUSTICS COLLOQUIUM
AACHENER AKUSTIK KOLLOQUIUM

Proceedings

November 27 – 29, 2017

Pullman Aachen Quellenhof

FEV fka HEAD acoustics® ITA RWTH AACHEN UNIVERSITY

Comprehensive model for the assessment of the NVH-behavior of electric vehicles

M. Müller-Giebeler[1], P. Drichel[2], M. Jaeger[3], J. Klein[1], Dr. M. Wegerhoff[4], S. Rick[3], Prof. Dr. M. Vorländer[1], Prof. Dr. G. Jacobs[2], Prof. Dr. K. Hameyer[3]

[1] *Institute of Technical Acoustics (ITA), RWTH Aachen University, Germany, Email: mmg@akustik.rwth-aachen.de*

[2] *Institute for Machine Elements and Machine Design (IME), RWTH Aachen University, Germany, Email: pascal.drichel@ime.rwth-aachen.de*

[3] *Institute of Electrical Machines (IEM), RWTH Aachen University, Germany, Email: markus.jaeger@iem.rwth-aachen.de*

[4] *Formerly: Institute for Machine Elements and Machine Design (IME), RWTH Aachen University, Germany; Currently: HEAD acoustics GmbH, 52134 Herzogenrath, Germany, Email: matthias.wegerhoff@head-acoustics.de*

Abstract

This contribution presents a hybrid model for the auralization and evaluation of the drive related interior noise in electric vehicles. The model combines the aspects of electromagnetic force excitation, structural-dynamic and subsequent acoustic response. The presented tool chain was first developed and implemented in the course of a joint project of three RWTH institutes and is currently extended and refined within a follow-up project between the same cooperation partners. The basic functions of the model are explained in the following and its application is illustrated for a given drive in a Smart Fortwo electric drive (model series 451). Simulation results are illustrated and ongoing work concerned with the advancement of the framework is discussed.

Introduction

The changing automotive market, which is characterized by a progressing electrification of vehicles, presents challenges with respect to the acoustic behaviour of powertrains. As indicated frequently, the characteristic noise of electric cars fundamentally differs from that of conventional drives [1]. Objective methods, obviating the need for expensive field tests to assess the passenger's perception of acoustic quality, have to be established. A simulation tool allowing for the prediction and assessment of the powertrain induced interior noise for various operating states, especially at an early stage of the design process, would considerably facilitate the development of electric drives. The development of such a tool was the objective of an interdisciplinary joint project, combining electromagnetic, structural-dynamic and acoustic sub-models, in order to provide an integrated method for the fast binaural auralization of an electrical drive train [2]. This paper illustrates the current state of the tool chain, as well as ongoing work focussed on the integration of additional aspects and the optimization of result quality versus computational effort.

Initial Implementation of the Simulation Model

General Structure of the Overall Model

The cross-domain simulation chain presented in Figure 1 uses a force excitation model for permanent magnet synchronous machine (PMSM) to initially calculate force densities on the stator teeth of the electrical machine. For computation of the structural-dynamic propagation, the powertrain is modeled in a multi-body-simulation, containing the electrical machine, gearbox and side shafts of the car. The previously determined electromagnetic forces and moments are

integrated into the simulation environment by application onto the elastic stator and rotor to calculate the resulting velocities and forces on the surface. In an intermediate step the sound field radiated from the machine is calculated using the supplied velocity distribution on the surface. The airborne and the structure-borne sound, captured by the force at the suspension points, are then transferred into the vehicle interior through measured binaural transfer paths and combined to form the audible ear signal. The modular structure of the tool chain allows developers to change individual properties of the modeled drive components to quickly assess the resulting auralized car cabin noise.

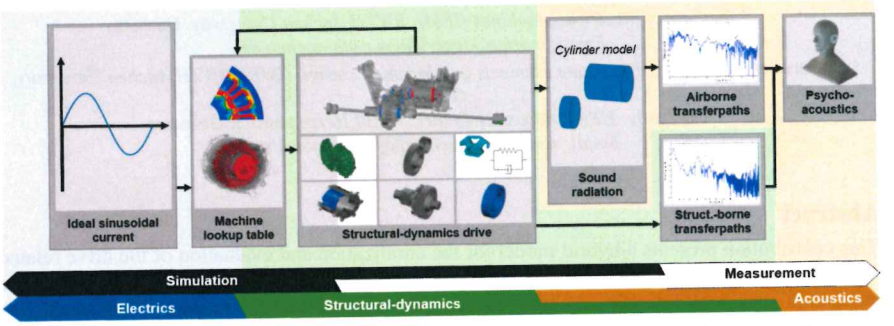

Figure 1: Schematic representation of the initial cross-domain tool chain and its sub-models.

Electromagnetics and Modelling of the Electrical Machine

As input for the structural dynamics drivetrain model the electromagnetic forces acting on the stator teeth and on the rotor are calculated. To achieve this, a simulation model is developed using a numerical approach based on the finite-element analysis (FEA). Some main machine parameters are gathered in table 1.

Symbol	Value	Unit	Description
N	36	-	Number of stator slots / teeth
p	6	-	Number of pole pairs
m	3	-	Number of phases
I_{ph}	0…300	A	Peak phase current
ψ	0…90	°	Control angle
ψ_{opt}	10	°	Control angle for nominal operating point
M	0…130	Nm	Torque of the electrical machine
n	0…12000	r/min	Speed of the electrical machine

Table 1: Main parameters for the permanent magnet synchronous machine.

Generally, in a PMSM the forces depend on the current described in the d-q-system with amplitude and control angle, as well as on the rotor position. To avoid the time consuming FEA computation at each time step, pre calculated values are gathered in a look-up-table (LUT), which is then used in the structural dynamic model. Therefore, rotor positions were varied in steps of 0.5°, control angle in steps of 5° and current amplitude in steps of 10 A. To cover every possibly occurring control angle in the rotor slices because of the skewed stator the actual range which needs to be computed is ±30° greater than the average control angle given in table 1.

The machine is modelled as partial 2D cross section including one pole pair. The skewing of the stator can be regarded as changed control angle along the axial machine length, and is taken into

account by the multi slice method [3]. The local force at every node of the mesh is calculated using the eggshell method [4].

The FEA shows that the forces at the tip of the tooth are dominant compared to the side of the tooth (see Figure 2, left). The average value of the tangential force is just about 5 to 10 % of the radial force (see Figure 2, right). Therefore the influence of the distribution of the tangential forces is neglected (modelled via the evenly distributed torque) and focus put to the radial forces.

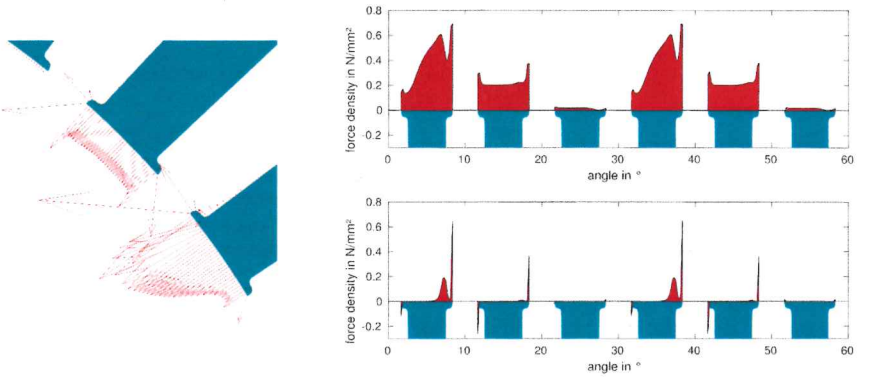

Figure 2: Forces on stator teeth for one rotor position, I = 110 A and ψ = 10°. Left: Nodal forces at stator teeth. Top right: Radial force density. Bottom right: Tangential force density.

With the discrete nodal forces known at each rotor position a Fourier transformation is performed. The LUT for the structural dynamic model contains the complex Fourier coefficients for the force density at the stator teeth in spatial and frequency orders, and the torque in frequency orders (see [5]).

Structural Dynamics

The structural dynamics NVH model is constructed in a Multi-Body Simulation framework (MBS) called SIMPACK [6]. It includes the drivetrain components electric machine with coolant, gearbox with differential and tooth meshing, side shafts, support arms, and subframe, all of which are modeled as elastic bodies. Elastomeric bushings and roller bearings are modeled as concentrated force elements. Groove and tapered roller bearings have load dependency by means of their stiffness. In addition to the previously described excitation with radial force and torque of the PMSM from the electric machine, a parametrized excitation of the gear stages with load- and angle-dependent stiffness characteristics for the tooth meshing are modeled as described in [7]. A geometrical representation of the structural drive train model is shown in Figure 3. (see [8],[9],[10])

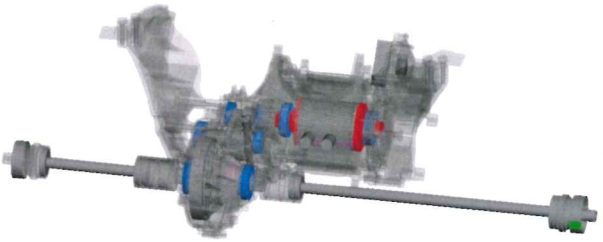

Figure 3: Drive train model with housing parts and support arms as one part elastic body, elastic shaft components, gears and bearings.

The structural behavior of the housing components as well as the behavior of the shafts is taken into account in an elastic manner with isotropic material properties. The validation of the modal representation of the housing components is done by comparing the eigenfrequencies and mode shapes. For quantification of the comparison between calculated and measured mode shapes the modal assurance criterion is used (see Eq. (1), [11]).

$$\mathrm{MAC(A,X)} = \frac{|\{\Psi_X\}^T\{\Psi_A\}|^2}{(\{\Psi_X\}^T\{\Psi_X\})(\{\Psi_A\}^T\{\Psi_A\})} \tag{1}$$

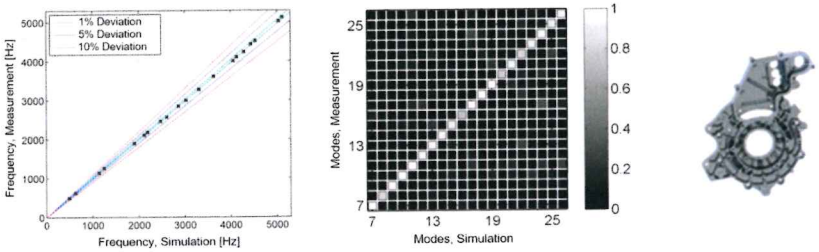

Figure 4: Exemplary comparison of eigenfrequencies (left) and modeshapes (center) of measurement and simulation for bearing shield of the electric machine (right) [5].

The isotropic material model does not describe the stator with its windings in sufficient quality. This problem can be overcome by using a transversally isotropic material model. It is characterized by the definition of two moduli of elasticity (E_p and E_t), two shear moduli (G_p and G_t) and the poisson's ratio ν_{pt}. (see Eq. (2), described in [10],[12])

$$\begin{Bmatrix} \varepsilon_{11} \\ \varepsilon_{22} \\ \varepsilon_{33} \\ \gamma_{12} \\ \gamma_{13} \\ \gamma_{23} \end{Bmatrix} = \begin{bmatrix} 1/E_p & -\nu_p/E_p & -\nu_{pt}/E_t & 0 & 0 & 0 \\ -\nu_p/E_p & 1/E_p & -\nu_{pt}/E_t & 0 & 0 & 0 \\ -\nu_{pt}/E_p & -\nu_{pt}/E_p & 1/E_t & 0 & 0 & 0 \\ 0 & 0 & 0 & 1/G_p & 0 & 0 \\ 0 & 0 & 0 & 0 & 1/G_t & 0 \\ 0 & 0 & 0 & 0 & 0 & 1/G_t \end{bmatrix} \cdot \begin{Bmatrix} \sigma_{11} \\ \sigma_{22} \\ \sigma_{33} \\ \tau_{12} \\ \tau_{13} \\ \tau_{23} \end{Bmatrix} \tag{2}$$

To parameterize the stator with winding model, an effective five step process has been developed. With this process the material properties of the characteristic equations of the described transversally isotropic material model are parametrized. This is possible because the mode shapes with and without shear, as well as the axial mode can be clearly identified in the

measurement results. The validation of the model in terms of eigenfrequencies and mode shapes shows a good match between measurement and simulation. The eigenfrequencies are within a tolerance band of ±5 %. (see Figure 5, [10])

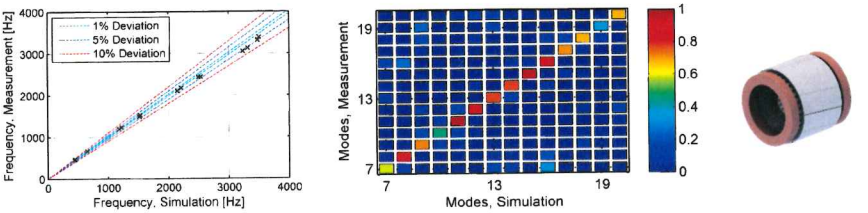

Figure 5: Comparison of eigenfrequencies (left) and mode shapes (center) of measurement and simulation of the stator with winding (right) [10].

Regarding the structural dynamic properties of the stator housing it has been shown that the coolant has to be taken into account. To include the coolant in the structural model of the stator housing, the model is extended by taking into account the fluid-structure-interaction. This is done by connecting the structural continuum finite elements and with additional acoustic fluid elements representing the coolant. This method takes into account the coupled dynamic mass and stiffness properties of structure and fluid. Results show similar characteristics between the simulation and measurements. [8]

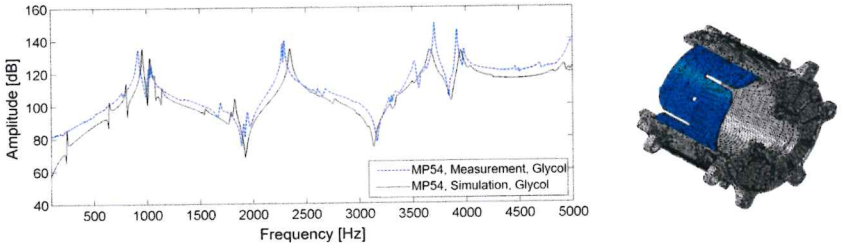

Figure 6: Comparison of measurement and simulation (left) for the fluid-filled stator housing of the electric machine (right) [8].

Acoustic Modeling

Interfaces between structural-dynamic and acoustic modeling

Processing of the structural results is done using two interfaces. The radiated airborne sound and the structure-borne sound are calculated based on the sampled surface velocity on the powertrain housing and the force at all coupling points between drive and vehicle structure respectively [13].

Airborne sound radiation

The objective of the radiation simulation is to determine the sound pressure signals in vicinity to the drive unit, which are then transferred to the driver's ears by means of airborne transfer paths. To efficiently calculate the airborne sound pressure from the surface velocities, stator and gearbox housing are approximated as cylindrical bodies with piston-shaped closing elements. Utilizing this approximation allows the application of an established analytical cylinder radiation

model [14], calculating the complex pressure in cylindrical coordinates based on the surface velocity spectrum

$$\underline{p}(r,\alpha,z) = \frac{1}{2\pi}\sum_{n=-\infty}^{\infty} e^{jn\alpha}\int_{-\infty}^{\infty}\underline{\bar{V}}(r_0,k_z)\frac{\underline{H_n}(k_r r)}{\underline{H_n'}(k_r r_0)}\,e^{jk_z z}\,dk_z \quad . \tag{3}$$

To verify the plausibility of the approach, the sound field results for a simple cylindrical body with the dimensions of the electrical machine were qualitatively compared with simulation results using the actual CAD-model of the stator housing in a boundary element method (BEM) simulation. Figure 7 depicts both calculation methods as well as one exemplary result for the same sine-shaped velocity distribution on the stator housing with a peak amplitude of 1 m/s (0. longitudinal- , 3. rotational mode) at a frequency of 4.5 kHz as input.

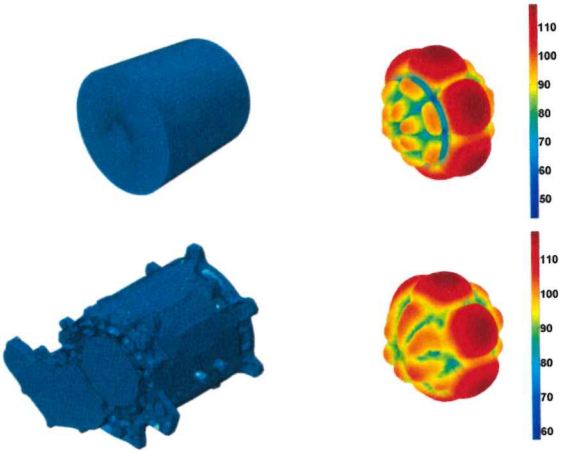

Figure 7: CAD-models and resulting sound pressure at 4.5 kHz on a radius of 2 m for the cylinder approximation (upper) and BEM simulation of the electrical machine (lower).

As the shape of the end plates covering gearbox and stator corresponds to a circular piston, their radiation can be calculated using analytical expressions for an ideal baffled circular piston. It is important to note that the individual contributions of the housings, the cover plates and the bearing shield to the overall radiation are initially computed separately and the resulting sound fields are superimposed afterwards.

Transfer paths

In order to get a realistic impression of drive modifications, it is necessary to evaluate the combined sound pressure at the position of the driver. Therefore, the quantities from the preceding simulation stages (the radiated airborne sound and the force at all bearing points) are convolved with measured binaural transfer paths, taking the structure-borne and airborne propagation adequately into account adequately.

Auralization and signal assessment

Using block-based processing, the surface velocity are transformed into the frequency domain by means of a short-time Fourier transform. After carrying out the cylinder- and piston simulation in the frequency domain, the signal blocks are transformed back into the time domain. The force

signals obtained from the structural simulation are high-pass filtered to remove the drive's static weight force and low-frequency transients. Subsequently the resulting time signals are convolved with the measured binaural transfer functions. The generated signals can be assessed by test subjects. In order to reduce the effort but still be able to assess the subjective perception, it is possible to evaluate a number of objectives as well as psychoacoustic parameters. So far, the signals were evaluated in terms of their spectrograms and their loudness.

Validation

Validation of the complex model chain was performed based on measurements of individual components, the entire power train, as well as through comparisons with real driving situations. Figure 8 for example, shows the comparison of the measured and the simulated waterfall diagram of an acceleration level in normal direction on a gearbox measurement point for partial load, respectively.

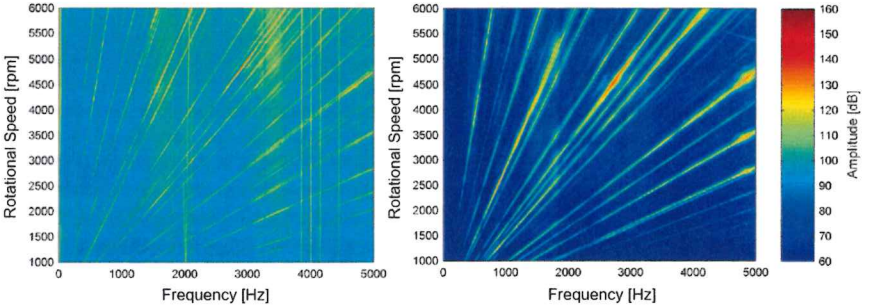

Figure 8: Comparison of waterfall diagrams between measurement (left) and simulation (right) [8].

The comparison indicates a plausible prediction of the exciting orders and similar levels between measurement and simulation. The fixed frequency shares at 2 kHz and 4 kHz in the measurement trace back to test-bed excitations. Also, binaural recordings of the interior noise during run-ups on a test track with the corresponding test car were carried out. Unfortunately, a direct comparison with auralized signals was hardly possible in this case. Powertrain related signals were strongly superimposed by noise, caused by additional influences such as rain, wind, tire rolling and vibration noises.

Application of the Comprehensive Model

In the following, results of a fully simulated run-up are shown for an experimental vehicle at partial load operation with 200A. All results refer to a powertrain consisting of PMSM and a two-stage single-speed transmission in a Smart Fortwo electric drive.

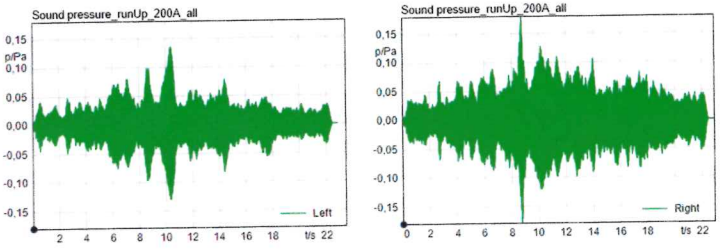

Figure 9: Temporal course of the sound pressure in Pa. Left driver's ear (left), right driver's ear (right).

Figure 9 shows the total resulting sound pressure at the driver's position, consisting of airborne and structure-borne noise shares. The resonance points at 2.6 seconds, 8.5 seconds and 10.4 second are clearly identifiable.

Besides a plausible auralization of powertrain induced noise as such, the purpose of the simulation chain is in particular the comparison of different design variants. Due to the modular structure of the toolchain with its dedicated sub-models, this is not only feasible for the eventually auralized pressure signal, but also for different influencing quantities that are computed during intermediate simulation steps. Following, this procedure is exemplarily described for the acceleration in normal direction at one point on the powertrain. Figure 10 shows the order level for the machine excitation (36^{th} + 72^{nd} order) over rotational speed with (brown curve) and without (red curve) the introduction of an elastic decoupling of rotor and gearbox shaft by integrating a flexible coupling component. The comparison between both simulation results shows, that the acceleration level due to a resonance in the range between 4000 rpm to 5000 rpm can be significantly reduced by this measure (level decrease of more than 20 dB).

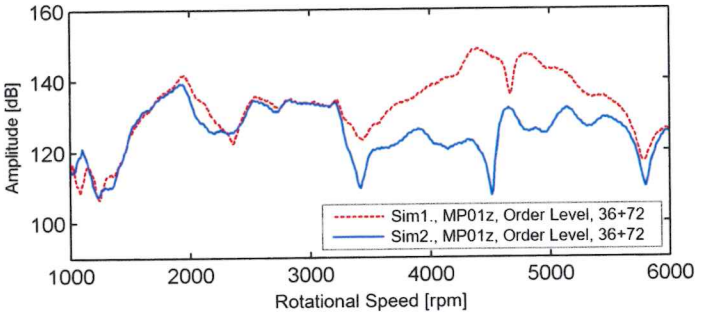

Figure 10: Simulated order level at one point prior to and after elastic decoupling of rotor and gear shaft.

Discussion and needs for Optimization and Expansion of the Model

In the previous section, the functionality of the model and its ability to efficiently simulate and auralize the drive induced interior noise were illustrated. The simulation chain allows the identification of dominant phenomena and the evaluation of measures through quick comparison of design variants. Nevertheless, the results gathered so far indicate further challenges regarding modeling level of details and implementation of the model. Results also indicate that additional physical aspects need to be incorporated into the simulation model and existing model parts must

be refined. Figure 11 illustrates the expansion of the model. Following, enhancements to the modeling method are discussed more in detail. To further validate the comprehensive simulation based on operational measurements, the interior noise will be recorded under reproducible conditions on the test track and on the dynamometer.

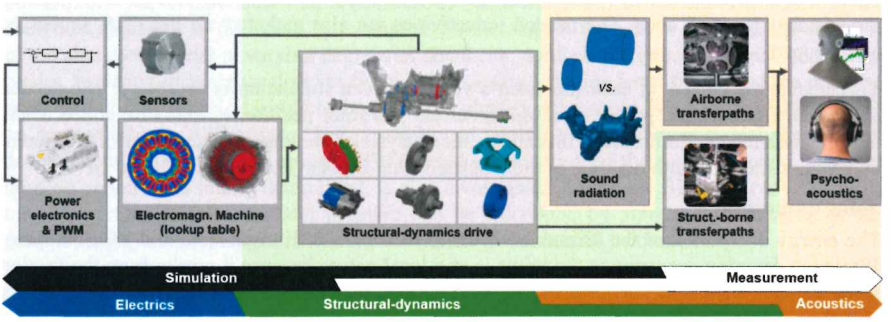

Figure 11: Schematic representation of the revised cross-domain tool chain and its sub-models.

Electrical system, current computation and interface

The presented feed forward approach includes a weak coupling between the structure dynamic and the electromagnetic model. The advantage is a relatively short simulation time for the LUT as well as the model itself while covering the most relevant effects. However, the complex retroactive phenomena between drive train, electrical machine, control and power electronics are little studied. To examine these effects a strongly coupled model computed in time domain is proposed.

The method for calculating the electromagnetic forces via 2D FEA, simulation of the 3-dimensional machine with the multi slice method and the LUT based approach shows good results and is kept. To represent eccentricities due to production deviations, rotor movement and deflections, the rotor position in two dimensions is added to the parameter variation. The amount of parameter combinations is reduced by taking advantage of every symmetry between operating points, eccentricity and geometry.

The description of the force density via complex Fourier coefficients showed to be memory consuming, and the back transformation to discrete forces at each time step computationally expensive. Since only one load application point per tooth and slice is used, the LUT is changed to discrete forces per tooth. This leads to lesser computational time and memory expenses. At first, this opens the possibility to add the additional two dimensions to account for the eccentricity of the rotor (see Table 2), and further more to map tangential and axial forces, as well as the torque at the tooth tip resulting from the summation of the nodal force vectors.

Parameter	Range	Unit	Description
I_{ph}	0…300	A	Current amplitude
ψ	-30…120	°	Control angle
φ	0…10	°	Rotor position angle (over one tooth/slot)
Ex_{tooth}	0…0,6	mm	Rotor excentricity in tooth direction
Ex_{slot}	0…0,6	mm	Rotor excentricity in slot direction

Table 2: Parameters to variate for force and inductivity computation via FEA.

Instead of an ideal sinusoidal current, the actual current as result of the machine inductivities and the pulse width modulation of the power electronics is used (see following section). The feedback from the structure dynamic model therefore consists of two parts. The controller gets the rotor angular position as it is measured by the resolver at its location, while the machine inductivities depend on the actual rotor position defined by angle and eccentricity (in two dimensions) for each slice. The needed inductivities are also gathered via the FEA, processed and mapped.

To compute the current at each time step a voltage driven simulation is necessary. The needed components (controller, power electronics, current and rotor position sensors) are added to the time domain model. Furthermore this allows the analysis of the impact of sensor errors, different controllers, the minimum off-time of the Insulated Gate Bipolar Transistors (IGBTs) etc.

Joint damping

The energy dissipation of the assembled housing parts results from material and joint damping. While the damping occurring at the joints is of a local nature because it results from the friction at the contact regions of the surfaces of the adjoining components, the material damping is of a global nature. It is distributed over each component. The joint damping is mainly responsible for the damping of structure-borne-sound in assembled structures. [15], [16]

In modelling the NVH behaviour of electric vehicles or drivetrains in general, the breakdown of global material and local joint damping is not yet state of the art. Instead, measured global modal damping values from similar constructions are frequently used. Often a constant degree of damping is defined for all modes. If prototypes are available, the damping can be determined experimentally and used to calibrate a model for a certain load level, which is also done in the structural dynamics model of the drivetrain described in this paper. However, since moderate changes in the geometry of components or in the load level can lead to severe fluctuations in the damping, a prediction of the damping of the assembly cannot be made with the method currently used.

In order to improve the predictability and to be able to estimate the effect of constructive changes in natural frequency, mode shape, and damping, the goal will be to take into account the global material and local joint damping separately.

Rubber joints

Data acquisition for engine mounts in the acoustically relevant frequency range for every spatial direction under preload is challenging. In further steps it is planned to identify the complex multi-axial-properties of the mount with measurements of the overall dynamic system properties of the drivetrain. Under the assumption that the properties of the drivetrain and its remaining components at the test-rig are well-known, the properties of the mounts are the only unknown quantities of the system. Therefore the properties can be extracted as transfer functions for one state of preload.

Figure 12: Used rubber joint as engine-transmission-mount.

Sound radiation model

To further validate the fast analytical approach it is intended to compare its results with a BEM simulation based on the complete model of the entire power train, which was not available during the first project period. The influence of more complex interactions between the powertrain's sub-components like reflections or shadowing, which are not considered in the analytical approach so far, could be evaluated. Furthermore it is possible to assess the accuracy of the analytical model in varying degrees of detail (i.e. number of frequency points, considered modes, radiation distance) and to verify the results using listening tests. In view of the practical application of the model, it would be beneficial to identify a threshold for modelling effort, based on the audibility of differences. The possibility of applying the analytical model during early development stages and then using a BEM-based computation of the radiated sound, once the housing geometry is finally determined, is also investigated. Using the BEM concept of acoutic transfer vectors (ATV), the field pressure can be calculated by simple multiplication of the constant and load-independent ATV-matrix with the given normal velocity vector

$$\boldsymbol{p} = [\boldsymbol{ATV}]_{mxn} \cdot \boldsymbol{v_n} \quad . \tag{4}$$

Since the ATV-matrix has to be computed once per frequency, the total effort for this approach especially depends on the required number of frequency points and has to be investigated for the issue at hand.

Psychoacoustics

Although the subjective assessment of a product sound is often influenced by the perceived loudness [17], sound quality is a complex perceptive attribute that is governed by various acoustic features. For a more differentiated evaluation of auralized signals, it is therefore reasonable to consider additional psychoacoustic parameters besides loudness. Especially parameters like sharpness and tonality are expected to prove beneficial in the context of electric vehicle noises with characteristic high frequency tonal components. Figure 13 shows the evaluation of sharpness and loudness for the simulated pressure signal already presented in Figure 9 (at the driver's left ear). Additional informational content is indicated by the deviation of both curves. The pronounced increase of the loudness at about 10.4 seconds is not paralleled by a corresponding shape of the sharpness because the loudness increase is mainly caused by low frequency resonances. Therefore the phenomenon might be perceived as less annoying despite the rise in loudness. Vice versa, the sharpness increases continuously with rising motor speed although the signal becomes quieter towards the end.

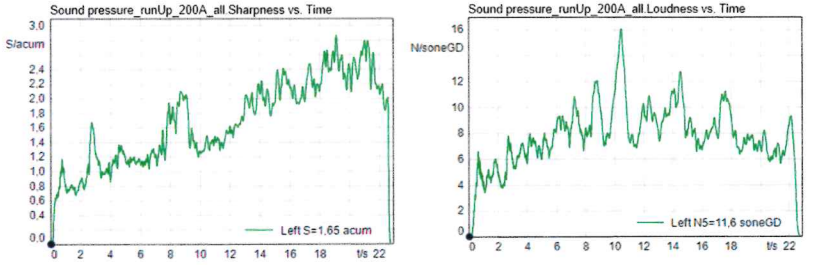

Figure 13: Sharpness versus loudness over time for the simulated pressure signal (run-up) at the left ear

The correlation between subjective assessments of electric vehicle interior noises and various psychoacoustic metrics is currently further investigated, as well as the potential development of a model for prediction of perceived quality based on these parameters.

Conclusions

The physically based model presented in this paper constitutes an efficient tool chain for the simulation and auralization of drive-related noise in electric vehicles. It is shown that dominant phenomena can be identified and rendered audible in a short time applying the tool chain presented. Although it already enables developers to freely change various properties of the drive and quickly assess the corresponding changes of the NVH characteristics, further enhancements to the tool chain, as well as further investigations regarding its precision, are needed and discussed in this contribution. The fundamental goal further model evolution will be to optimize the tool chain compromise between result quality and computational efficiency.

Acknowledgment

This work is based upon a collaboration between three institutes of RWTH Aachen University: Institute of Technical Acoustics (ITA), the Institute for Machine Elements and Machine Design (IME) and the Institute of Electrical Machines (IEM). The corresponding research projects No. 682-I and 682-II are organized in Forschungsvereinigung Antriebstechnik e. V. (FVA) in Germany and funded by AiF in the frame of the program of Industrielle Gemeinschaftsforschung (IGF) by Federal Ministry for Economic Affairs and Energy (BMWi). The corresponding authors appreciate the funding of the projects.

References

[1] Eisele, G.; Genender, P.; Wolff, K.; Schürmann, G.; Electric vehicle sound design – just wishful thinking? Aachen Acoustics Colloquium 2010.

[2] Rick, S.; Wegerhoff, M.; Klein, J.; E-MOTIVE NVH-Simulationsmodell - Modellbildung zur NVH Simulation eines E-MOTIVE Antriebsstrangs, FVA 682 I, Abschlussbericht, Frankfurt, 2015.

[3] Schlensok, C.; van Riesen, D.; Seibert, D.; Hameyer, K.; Fast structuredynamic simulation of electrical machines using 2D-3D-coupling, In: Proc. 6th Int. Conf. Comput. Electromagn., 2006, pp. 1-2.

[4] Henrotte, F.; Hameyer, K.; A theory for electromagnetic force formulas in continuous media, In: IEEE Transactions on Magnetics, vol. 43, no. 2, Apr. 2007, pp. 1445–1448.

[5] Rick, S; Putri, A. K.; Franck, D.; Hameyer, K.; Hybrid acoustic model of electric vehicles: Force excitation in permanent magnet synchronous machines, In: USB Proceedings 2015 IEEE International Electric Machines and Drives Conference (IEMDC), Coeur d'Alene, 2015.

[6] Simpack AG; Documentation, Force Element Catalogue, 2010.

[7] Andary, F.; Wegerhoff, M., Piel, D.; MBS Gear-tooth Stiffness Model - Implementation of a new coupling model for fast and accurate simulation of gear pairs using stiffness characteristic arrays. In: International Conference on Gears, 2015.

[8] Wegerhoff, M.; Methodology for the Numerical NVH Analysis of an Electrified Passenger Vehicle Drive Train, Verlagsgruppe Mainz GmbH, ISBN: 978-3-95886-167-1, Aachen, 2017.

[9] Wegerhoff, M.; Schelenz, R.; Jacobs, G.; Hybrid NVH Simulation for Electrical Vehicles II - Structural Model. In: Becker S (ed.) Fortschritte der Akustik: DAGA 2015, Nürnberg ; 16. - 19. März 2015; 41. Jahrestagung für Akustik ; Tagungsband. Berlin: Dt. Ges. für Akustik, 2015.

[10] Wegerhoff, M.; Drichel, P.; Back, B.; Schelenz, R.; Jacobs, G.; Method for determination of transversely isotropic material parameters for the model of a laminated stator with windings. In: 22nd International Congress on Sound and Vibration. Florence, p. 8, 2015.

[11] Ewins, D.; Modal testing. Theory practice and application. 2. ed. Baldock: Research Studies Press, 2000.

[12] Altenbach, H.: Kontinuumsmechanik. Einführung in die materialunabhängigen und materialabhängigen Gleichungen. 3., überarb. Aufl. 2015. Berlin, Heidelberg: Springer Berlin Heidelberg, 2015.
[13] Klein, J.; Behler, G.; Vorländer, M.; Hybrid NVH Simulation for Electrical Vehicles III - Acoustic Model. In: Becker S (ed.) Fortschritte der Akustik: DAGA 2015, Nürnberg ; 16. - 19. März 2015; 41. Jahrestagung für Akustik ; Tagungsband. Berlin: Dt. Ges. für Akustik, 2015.
[14] Williams, E. G.; Fourier acoustics: Sound radiation and nearfield acoustical holography. Academic Press, 1999.
[15] Werkstoff- und Bauteildämpfung - Dämpfung von Baugruppen (Blatt 3), Verband Deutscher Ingenieure (VDI), 2004.
[16] Möser, M.; Kropp, W.; Körperschall. Physikalische Grundlagen und technische Anwendungen. 3., aktualisierte Aufl. Heidelberg, New York: Springer, 2010.
[17] Blauert, J.; Commuication Acoustics. Berlin, Heidelberg, New York: Springer, 2005.